Table S1. Driver variables were developed by the following groups of authors (Lecky 2016, Wedding et al. 2018, Donovan et al. 2023) and their methods are summarized here. Drivers were standardized to a spatial resolution of 100 meters for analysis according to the methods of (Donovan et al. 2023).

Drivers		**Units**	**Description**	**Data Source**
Land-Based Pollution Drivers	Urban Runoff	Area of impervious surface per watershed	Modeled as a proxy by calculating impervious surfaces using NOAA Coastal Change Analysis Program (CCAP) high resolution land-use land-cover per watershed and then extending these values offshore. Includes trash, household chemicals, oil from roads, and other forms of urban runoff.	(Lecky 2016)
	Golf course runoff	Area of golf courses per watershed	Pesticides and fertilizers were modeled as a proxy using subsets from CCAP 'open developed space', then validated using Google Earth and ESRI imagery to calculate golf course area per watershed. These values were extended offshore.	(Lecky 2016)
	Agricultural runoff	Area of agricultural runoff per watershed	Pesticides and fertilizers from agricultural runoff were modeled as a proxy by using CCAP to calculate the area of agricultural land per watershed. These values were extended offshore.	(Lecky 2016)
	Coastal habitat modification	Presence of habitat modifying features	Direct alteration, removal, and destruction of habitat including coastal engineering (ex. seawalls, piers), dredging, and offshore aquaculture were consolidated, modification was represented as presence/absence.	(Lecky 2016, Wedding et al. 2018)
	Sedimentation	Average annual amount of sediment (tons/year)	Annual average delivery of sediment offshore was estimated using the Integrated Valuation of Ecosystem Services and Tradeoffs (InVEST) sediment delivery ratio model.	(Lecky 2016, Wedding et al. 2018)

	On-site waste disposal	g/day and effluent in gallons a day	Estimated nutrient flux from on-site waste disposal systems (cesspools, septic tanks). Nutrient flux was estimated by land parcel from the Hawai‘i Department of Health and by proximity to individual systems.	(Lecky 2016, Wedding et al. 2018)
Fishing Drivers	Non-commercial boat-based spear	Kg/ha	Island-scale annual average non-commercial boat-based reef fisheries catch from spear were calculated from the Marine Recreational Information Program (MRIP) data. Values were mapped offshore by modeling the distance to harbors, boat launches, human population within 30km, and managed area regulations.	(Lecky 2016, Wedding et al. 2018, McCoy et al. 2018)
	Non-commercial shore-based line	Kg/ha	Island-scale annual average non-commercial boat-based reef fisheries catch from line were calculated from the MRIP data. Values were mapped offshore by modeling shoreline accessibility using TIGER roads, USGS DEM slope, managed area regulations, and gear-specific spatial footprints.	(Lecky 2016, Wedding et al. 2018)
	Non-commercial shore-based net			
	Non-commercial shore-based spear			
	Aquarium Collection	#/ha	Average annual reported commercial aquarium catch by reporting block from the Hawai‘i Division of Aquatic Resources.	(Lecky 2016)
	Commercial line	Kg/ha	Average annual commercial catch of reef fish species with line gear type by reporting block from Hawai‘i Division of Aquatic Resources.	(Lecky 2016, Wedding et al. 2018)
	Commercial spear			
	Boat-based net	kg/ha	Summed annual catch of commercial and non-commercial boat-based catch of reef fish species by net, (according to commercial reporting methods and non-commercial boat-based estimates described above).	(Lecky 2016, Wedding et al. 2018, McCoy et al. 2018)
Physical	Chlorophyll-*a* anomaly maximum	mg/m3	Created using 4 km MODIS, 8-day composites.	(Gove et al. 2013, Wedding et al. 2018)

	Chlorophyll-*a* anomaly frequency	mg/m3	Created using 4 km MODIS, 8-day composites.	(Gove et al. 2013, Wedding et al. 2018)
	Chlorophyll-*a* long term mean	mg/m3	Created using 4 km MODIS, 8-day composites.	(Gove et al. 2013, Wedding et al. 2018)
	Temperature standard deviation	℃elsius	Sea surface temperature created from weekly NOAA blended satellite imagery (NOAA Pathfinder, NOAA/NEDIS/STAR), represents variability associated with regime.	(Gove et al. 2013, Wedding et al. 2018)
	Wave anomaly maximum	KW/m	From .5–1 km hourly data from the Simulating Waves Nearshore (SWAN) model from 2000-2013.	(Gove et al. 2013, Wedding et al. 2018)
	Wave anomaly frequency	KW/m	From .5–1 km hourly data from the Simulating Waves Nearshore (SWAN) model from 2000-2013.	(Gove et al. 2013, Wedding et al. 2018)
Habitat Drivers	Complexity	Topographic rugosity, slope of slope	Combined slope of slope from 1999–2001 LiDAR surveys conducted by the Army Corps of Engineers (SHOALS), LiDAR surveys conducted by Army Corps of Engineers in 2013 (CZMIL), and imaging spectroscopy data from Arizona State's Global Airborne Observatory(Asner et al. 2020).	(Donovan et al. 2023)
	Depth	Meters	Created from in situ surveys, 1999–2001 LiDAR surveys conducted by the Army Corps of Engineers (SHOALS), LiDAR surveys conducted by Army Corps of Engineers in 2013 (CZMIL), and imaging spectroscopy data from Arizona State's Global Airborne Observatory (Asner et al. 2020).	(Donovan et al. 2023)
	Habitat Type – Coral, Pavement, Boulder, Unknown	N/A	Based on maps produced by NOAA's Biogeography Branch. Four habitat types were included—reef (coral dominated hard bottom), pavement, boulder, and other hardbottom (unknown).	(Battista et al. 2007, Donovan et al. 2023)

Table S2. Model fit and predictive accuracy measures from three models of *Acanthurus achilles* presence and absence and 27 predictors. Marginal R^2 indicates the amount of the variation accounted for by the model excluding random effects, while Conditional R^2 includes the variation accounted for by the random effects. Difference in deviance is the deviance of a null model (intercept-only with no predictors while retaining the random effects) minus the deviance of the model with all predictors, where a difference greater than 54 (2*number of predictors) indicates a significant improvement in fit. Classification error rate is the percentage of the observed data that was correctly classified as present or absent under the model prediction using a probability cut off of 0.5, 0.7, or 0.9.

	Full Model	Adult Model	Juvenile Model
Marginal R^2	0.415	0.464	0.439
Conditional R^2	0.621	0.554	0.662
Difference in deviance (null model – fitted model)	219.57	155.82	100.26
Classification error rate, $p > 0.5$	92.3%	96.6%	95.0%
Classification error rate, $p > 0.7$	91.7%	96.7%	94.1%
Classification error rate, $p > 0.9$	90.9%	96.7%	93.2%

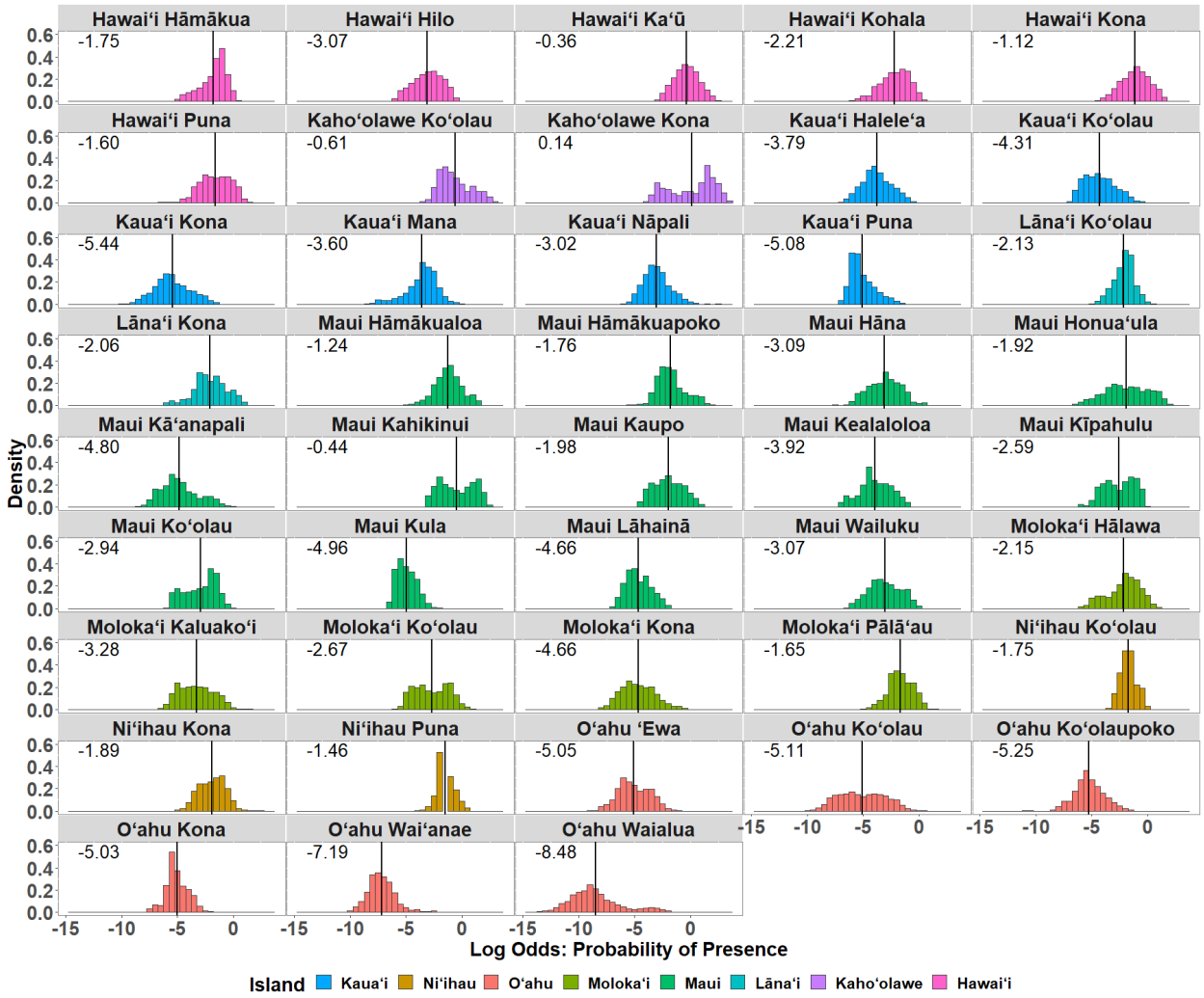

Figure S1. Density of log-odds probability of *Acanthurus achilles* presence per moku (see Figure 1 for map of moku boundaries). The x-axis is the log odds probability of *A. achilles* presence and the y-axis is the density for each of the bins on the x-axis. The black vertical line represents the mean value of the log odds probability of presence and is labeled in the upper left corner of each plot.

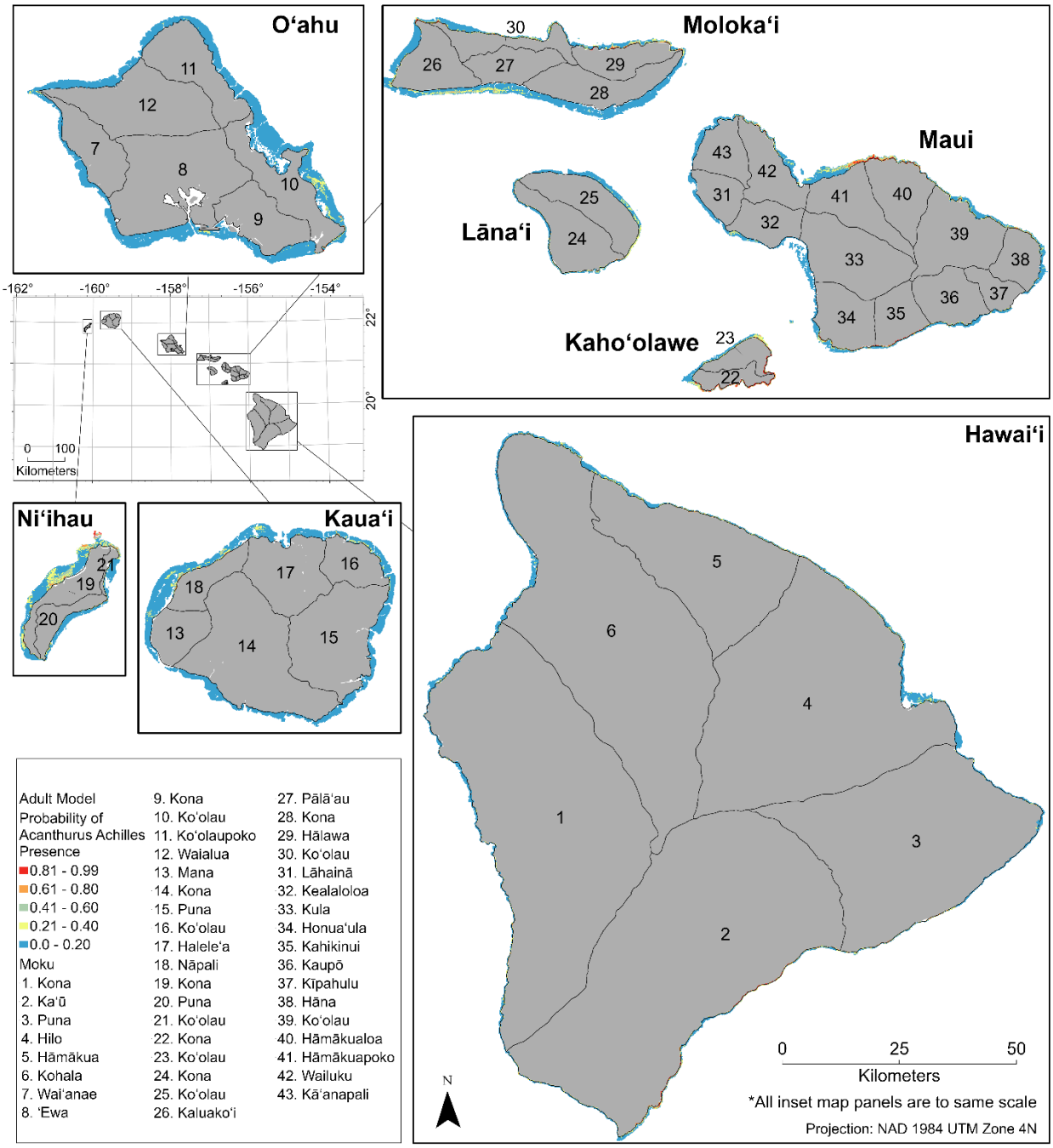

Figure S2. Map of predicted probability of *Acanthurus achilles* presence based on model with 27 drivers for adult individuals for the entire study extent. Areas in blues and yellows indicate lower probability of presence, and areas in red and orange represent higher probabilities of presence. Black lines on land are moku boundaries, delineations used in traditional forms of resource management in Hawai'i, where numbers correspond to moku names in legend.

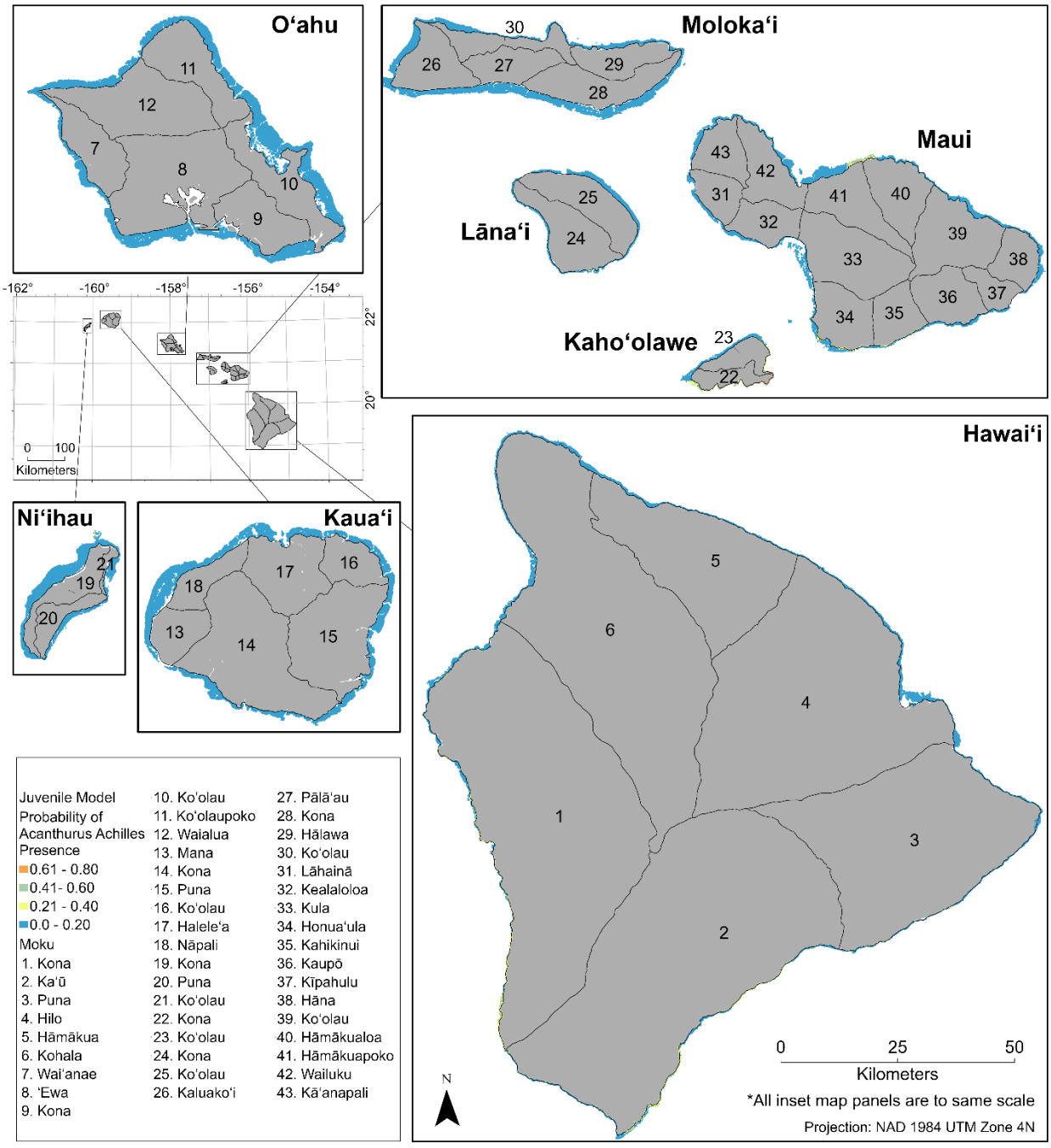

Figure S3. Map of predicted probability of *Acanthurus achilles* presence based on model with 27 drivers for juveniles for the entire study extent. Areas in blues and yellows indicate lower probability of presence, and areas in red and orange represent higher probabilities of presence. Black lines on land are moku boundaries, delineations used in traditional forms of resource management in Hawai'i, where numbers correspond to moku names in legend.

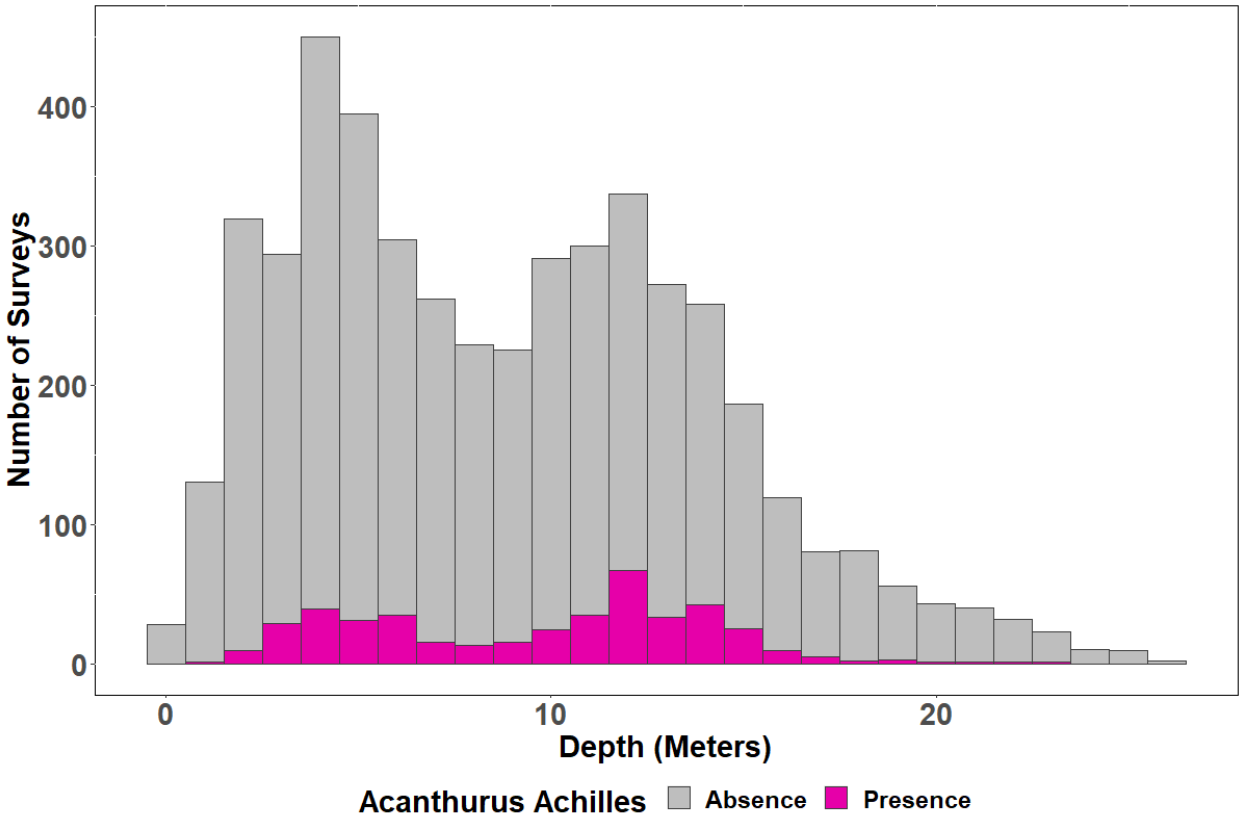

Figure S4. Density plot of the depths of *in-situ* fish surveys. The x-axis represents the depth in meters at the site where the survey was conducted and the y-axis shows the number of surveys. The bars are shaded according to the presence or absence of *Acanthurus achilles* at a given survey location – grey indicates absence and pink indicates presence.

Literature cited:

Asner GP, Vaughn NR, Balzotti C, Brodrick PG, Heckler J (2020) High-Resolution Reef Bathymetry and Coral Habitat Complexity from Airborne Imaging Spectroscopy. Remote Sensing 12:310.

Battista T, Costa B, Anderson S (2007) Shallow-water benthic habitats of the main eight Hawaiian Islands (DVD). NOAA Tech. Memo. NOS NCCOS 61.

Donovan MK, Counsell CWW, Donahue MJ, Lecky J, Gajdzik L, Marcoux SD, Sparks R, Teague C (2023) Evidence for managing herbivores for reef resilience. Proc R Soc B 290:20232101.

Gove JM, Williams GJ, McManus MA, Heron SF, Sandin SA, Vetter OJ, Foley DG (2013) Quantifying Climatological Ranges and Anomalies for Pacific Coral Reef Ecosystems. PLoS ONE 8:e61974.

Lecky J (2016) Ecosystem vulnerability and mapping cumulative impacts on Hawaiian reefs. MS thesis, University of Hawaii at Manoa, Honolulu, HI.

McCoy KS, Williams ID, Friedlander AM, Ma H, Teneva L, Kittinger JN (2018) Estimating nearshore coral reef-associated fisheries production from the main Hawaiian Islands. PLoS ONE 13.

Wedding LM, Lecky J, Gove JM, Walecka HR, Donovan MK, Williams GJ, Jouffray JB, Crowder LB, Erickson A, Falinski K, Friedlander AM, Kappel CV, Kittinger JN, McCoy K, Norström A, Nyström M, Oleson KLL, Stamoulis KA, White C, Selkoe KA (2018) Advancing the integration of spatial data to map human and natural drivers on coral reefs. PLoS ONE 13.